Journal of Multidisciplinary Engineering Science Studies (JMESS)
ISSN: 2458-925X
Vol. 10 Issue 5, May - 2024

Rock-carrying Flow Field Numerical Simulation of Rock Debris Bed Remover in Horizontal Well

Xu Zheng, Jinwu Luo, Gui Xu
School of Intelligent Manufacturing
Chengdu Technological University
Chengdu, China
ljwcdtu@163.com

***Abstract*—The rock-carrying flow field of the rock debris bed remover is complex and variable. To reduce the cost of experimental research and obtain a reasonable design basis, the rock-carrying flow field of the rock debris bed remover is analyzed and studied based on the numerical simulation technology using the liquid-solid two-phase flow model. The results show that the spiral structure of the rock debris bed remover has obvious rotary excavation and accelerated rock debris transportation, which can directly damage the rock debris bed and improve the rock-carrying performance of the flow field in the bottom of the well. Rock-carrying flow field numerical simulation is an efficient and intuitive means of analysis, which provides a reference for the design and optimization of the rock debris bed remover.**

Keywords—flow field numerical simulation; rock debris bed remover; rock-carrying performance

I. INTRODUCTION

Horizontal well drilling technology is an important technical means for oil extraction, and this technology faces many challenges in the process of implementation. Among them, the accumulation of rock debris bed will form drilling resistance to the drilling tools, reduce drilling efficiency, and in serious cases, downhole safety accidents such as stuck drilling and held drilling will occur, which will bring huge economic losses. At present, the design of rock debris bed remover has become one of the most promising research directions. However, the complexity and variability of bottomhole conditions in horizontal wells have led to difficulties in theoretical research and increased costs in experimental research. The application of numerical simulation technology can effectively solve the above problems. In this paper, a numerical simulation study of the rock-carrying flow field in the bottomhole of a spiral-type rock debris bed remover is carried out. Based on the CFD-DEM coupling technique, the interactions between the rock debris and drilling fluids, the rock debris, and the solid wall surface are taken into account. An analytical model and a methodology about the flow field of rock debris bed remover in horizontal well are built, which lays a foundation for the structural design and optimization of the subsequent tools.

II. FLOW FIELD SIMULATION THEORY

Neglecting the heat transfer and loss, the flow field of rock debris bed remover in horizontal well follows two basic laws: conservation of mass and conservation of momentum. The flow field mainly consists of drilling fluid in continuous phase and rock debris in discrete phase, which interact with each other to form the rock-carrying flow field.

The drilling fluid at the bottom of the well is in turbulent flow during the normal operation of the rock debris bed remover. The simulation of the drilling fluid is realized by using the realizable *k-e* turbulence model in CFD technology, in which the turbulent viscosity coefficient μ_t is described by a function of the turbulent kinetic energy k and the dissipation rate ε, with the expression,

$$\mu_t = C_\mu \rho \frac{k^2}{\varepsilon} \tag{1}$$

The expressions for the turbulent kinetic energy k and the dissipation rate ε for this model are of the following form:

$$\rho \frac{dk}{dt} = \frac{\partial}{\partial x_i}\left[\left(\mu + \frac{\mu_t}{\sigma_k}\right)\frac{\partial k}{\partial x_i}\right] + G_k + G_b - \rho\varepsilon - Y_M \tag{2}$$

$$\rho \frac{d\varepsilon}{dt} = \frac{\partial}{\partial x_i}\left[\left(\mu + \frac{\mu_t}{\sigma_\varepsilon}\right)\frac{\partial \varepsilon}{\partial x_i}\right] + \rho C_1 S\varepsilon - \rho C_2 \frac{\varepsilon^2}{k + \sqrt{v\varepsilon}} + C_{1\varepsilon}\frac{\varepsilon}{k} C_{3\varepsilon} G_b \tag{3}$$

Where, ρ is the fluid density, kg/m^3. G_k is the turbulent energy generation caused by the average velocity gradient. G_b is the turbulent energy generation caused by the buoyancy effect. Y_M is the compressible turbulence pulsation expansion on the total dissipation rate. σ_k is the turbulence Platt's number of the turbulent energy, generally taken as 1.2. σ_ε is the turbulence Platt's number of the dissipation rate, generally taken as 1.0. C_1 is a value of the constant,

generally taken as 1.9. C_2 is a value of the constant, generally taken as 1.44.

The rock debris bed in the flow field at the bottom of a horizontal well consists of countless rock particles deposited and accumulated. The contact behaviors between the rock debris and the rock debris, and between the rock debris and the solid wall are simulated by using the Hertz Mindlin no-slip contact model of the DEM technique [1], [2]. The rolling resistance mechanical model is introduced to characterize the mechanical state of rock debris during rolling [3], with the expression,

$$M_r = \frac{-\omega_{rel}}{|\omega_{rel}|} C_r R_{eq} F_n \quad (4)$$

$$\omega_{rel} = \omega_1 - \omega_2 \quad (5)$$

$$R_{eq} = \frac{1}{\frac{1}{R_1} + \frac{1}{R_2}} \quad (6)$$

Where M_r is the rolling damping moment, N·m. ω_{rel} is the relative rotational angular velocity, rad/s. C_r is the rolling friction coefficient. F_n is the contact normal force, N. R_{eq} is the equivalent radius of the two spherical rock debris particles, m. ω_1 and ω_2 are the rotational angular velocities of the spherical rock debris particles 1 and 2, rad/s. R_1 and R_2 are the radius of the spherical rock debris particles 1 and 2, m. For the solid wall surface in contact with the rock debris, the rotational angular velocity is 0 and the radius is infinity.

The interaction between rock debris and drilling fluid is realized by CFD-DEM coupling. The coupled interaction force model contains models of trailing force, rotational lift, shear lift, pressure gradient force, virtual mass force, centrifugal force, Coriolis force, and Basset force.

III. NUMERICAL SIMULATION METHODS

A. *Geometric modeling of wellbore flow field*

Taking the double screw type rock debris bed remover with a nominal diameter of 127 mm as the research object, the modeling was established as shown inFig.1. The core structure of this debris bed remover mainly consists of a flow removal zone and a corrective support zone.

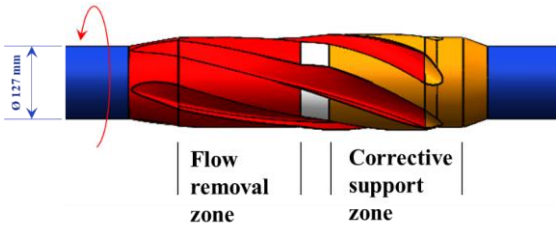

Fig.1. Geometric model of a spiral rock debris bed remover

The wall surface of the bottom of the horizontal well is simplified as a cylindrical surface with a diameter of 215.9 mm, and the Boolean subtraction operation function in the 3D modeling software is used to establish the geometric model of the computational domain of the rock-carrying flow field of the rock debris bed remover, as shown in Fig. 2. The overall computational domain is divided into two parts, the rotating region and the stationary region. The computational information will be transferred between the two regions through the data exchange surface. Due to gravity, the rock debris bed remover is offset along the direction of gravity, and it is assumed that the offset is 11.37 mm.

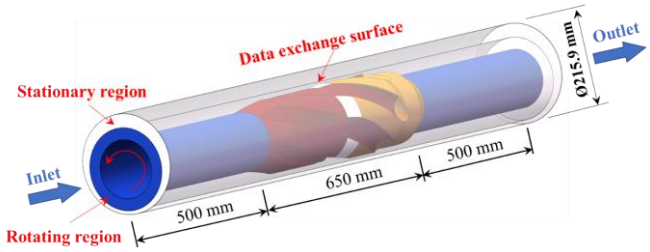

Fig.2. Geometric model of the computational domain of the rock-carrying flow field of the debris bed remover

B. *Physical modeling*

A horizontal well with a depth of 4000 m and a pumping pressure of 20 MPa was used as the simulated working condition. The density of drilling fluid was taken as 1000 kg/m^3, and the dynamic viscosity was 0.00089 Pa·s, and the drilling fluid volume flow rate was 30 L/s.

The rotational speed of the drilling tool was set to 60 r/min, and the mechanical drilling speed was assumed to be 10 m/h. At this mechanical drilling speed, the volumetric generation rate of the rock debris at the bottom of the well was 1.016×10-4 m3 /s, and the generated rock debris go upward with the drilling fluid and pass through the rock debris bed remover. Considering the complexity of the wellbore environment and the uncertainty of the rock debris state, several assumptions were made: 1) assuming that the rock debris are spherical particles; 2) assuming that the mechanical properties of a single rock debris are isotropic; 3) assuming that the rock debris are uniformly injected from the inlet; and 4) assuming that the injection rate of the rock debris at the inlet is equal to the inflow rate of the drilling fluid. Based on the assumptions, the rock debris parameters are set asTable1.

Table1. Parameters of rock debris

Parameters	Value
Density / (kg·m^{-3})	2500
Young's modulus / MPa	15000
Poisson's ratio	0.25
Coefficient of static friction between rock debris and rock debris	0.61
Coefficient of rolling friction between rock debris and rock debris	0.01
Coefficient of normal elastic recovery of rock debris	0.50
Coefficient of tangential elastic recovery of rock debris	0.50
Coefficient of static friction between rock debris and wall	0.70
Coefficient of rolling friction between rock debris and wall	0.02
Coefficient of normal elastic recovery between rock debris and wall	0.50
Coefficient of tangential elastic recovery between rock debris and wall	0.50

C. Boundary conditions

(1) The inlet condition is velocity inlet.

(2) The outlet condition is pressure outlet.

(3) The rock debris remover wall conditions are kinematic no-slip boundaries.

(4) The wellbore wall is a fixed no-slip boundary.

(5) There is no heat transfer or penetration between the drilling fluid, rock debris, and walls. The direction of gravity is downward perpendicular to the axial direction of the wellbore.

D. Description of the solution

According to the experience of CFD-DEM coupling in other fields, based on the Rayleigh time-step criterion [4], the time-step ratio of the DEM solver is set to be 0.2, which corresponds to a time-step of the DEM solver of about 0.00001 s. The time-step of the CFD transient solver is set to be 0.001 s. Under the working conditions set in the preceding section, the physical time of the numerical simulation reaches 2 s when the computation converges completely, the rock-carrying flow field is in a dynamic equilibrium state.

IV. ANALYSIS OF SIMULATION RESULTS

A. Rock debris distribution

Fig. 3 shows the distribution of rock debris at the moment of 2 s. At this time, the calculation is completely converged, the rock debris distribution in the calculation domain is in the state of dynamic equilibrium, and the distribution and transportation velocity of rock debris in each place tends to be stabilized. When the drilling fluid volume flow rate is 30 L/s and the rotational speed of drilling tool is 60 r/min, the rock debris distribution in each zone shows different states. The rock debris in the inlet zone are more evenly dispersed in various positions in the annulus, and the rock debris transportation velocity is around 1.2~1.56 m/s. The rock debris in the flow removal zone and corrective support zone are also dispersed at various locations in the annulus, but the overall distribution is slightly lower, and the rock debris transportation velocity is around 1.38~2.37 m/s. The rock debris in the outlet zone area basically settled at the bottom with lower transportation velocity about 0.305~1.2 m/s.

Comprehensively, under the influence of gravity, the rock debris entering the flow field settle downward along the axial path as a whole, eventually forming a rock debris bed. The spiral structure of the rock debris bed remover can obviously prevent or even destroy the formation of the rock debris bed, and enhance the transport effect on the velocity of the rock debris, so that the rock debris have the maximum transport velocity in the working zone of the rock debris bed remover.

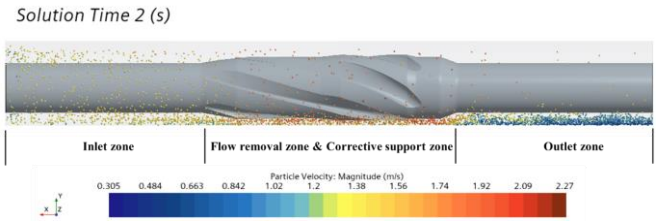

Fig. 3. Overall distribution of rock debris during dynamic equilibrium (30 L/s, 60 r/min)

B. Rock debris retention

The rock debris retention is the total mass of rock debris present in the simulation calculation area, and the curve of rock debris retention with time can characterize the removal efficiency of rock debris [5]. The variation curves of the rock debris retention under simulated conditions using the rock debris bed remover and conventional drill pipe are given in Fig. 4. In the first stage of simulation (0~0.1 s), no rock debris is generated and the rock debris retention is 0. In the second stage of simulation (0.1~2 s), the rock debris continuously flow into the computational domain from the inlet with a mass flow rate of 0.254 kg/s. In the second stage, the rock debris retention increases linearly with time at first, and with the outflow of rock debris from the outlet and the outflow amount is lower than the inflow amount, the rock debris retention shows a curved curve with a decreasing slope, and finally the outflow of the rock debris is basically the same as the inflow amount, and the rock debris retention is in a dynamic equilibrium and maintained at a stable value.

Fig. 4 shows that the curve corresponding to the rock debris bed remover changed from linear to curved earlier, indicating that the use of the rock debris bed remover accelerated the discharge of rock debris toward the outlet. Under the working condition of 30 L/s displacement and 60 r/min rotation speed, the final rock debris retention of the conventional drill pipe is maintained at about 0.3247 kg, while the final rock

debris retention of the rock debris bed remover is reduced to about 0.3171kg, with a reduction of 2.34%. So, the rock debris bed remover improved the efficiency of rock debris removal in horizontal wells.

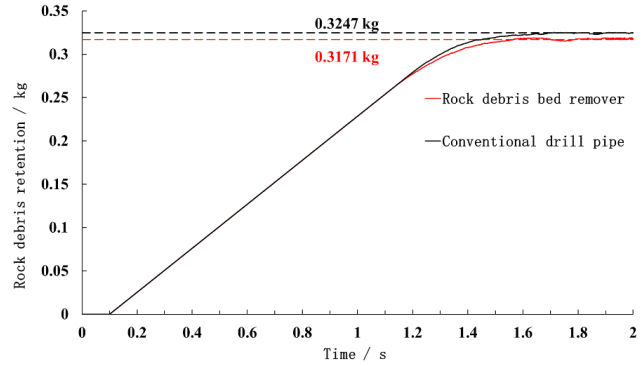

Fig. 4. Variation curve of rock debris retention with time using different tools (30L/s, 60r/min)

C. Axial transport velocity of rock debris

The axial transport velocity of rock debris can visualize the trend of rock debris flow to the outlet and characterize the rock-carrying performance of the flow field, and the larger the value, the better the rock-carrying performance. In order to more intuitively reflect the rock-carrying performance, based on the Lagrange particle tracking method, eight cross sections in the flow field region (Fig. 5) were analyzed for the average axial transport velocity of rock debris. The average axial transport velocity of rock debris in each cross-section is analyzed by the equation

$$\overline{v}_{n-n} = \frac{\sum_{i=1}^{S} v_{i,n-n}}{S} \tag{7}$$

Where, $\overline{v}_{n-n}$ is the average axial transportation velocity of rock debris passing through section *n*, m/s; S is the total number of all rock debris particles; $v_{i,n-n}$ is the axial transportation velocity of the rock debris particle *i* passing through section *n*, m/s.

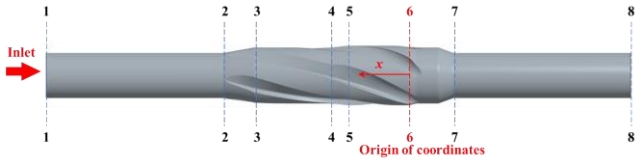

Fig. 5. Eight cross sections used to analyze the average axial transport velocity of rock debris

Fig. 6 shows the average axial transport velocity of rock debris in 8 sections under analyzed working conditions. The overall axial transport velocity of rock debris shows a trend of increasing and then decreasing. Among them, the structure of the rock debris bed remover at cross-section 2-3 has a sudden expansion, and the decrease of the overflow area makes the rock debris transportation velocity increase faster. The structure of the rock debris bed remover at cross-section 6-7 has a sudden contraction, and the increase of the overflow area makes the rock debris transportation velocity decrease faster. In comparison, when the rock debris enters into the outlet zone between cross-section 7-8, its transportation velocity decreases faster, and its performance of rock-carrying performance is the worst. Overall, the greater transport velocity between sections 3 and 6 indicate that the core functional zone of the debris bed remover has the best rock-carrying performance.

The comprehensive analysis concluded that the rock debris bed remover can not only destroy the generation of rock debris bed, but also directly enhance the rock-carrying performance of the flow field at the bottom of the well.

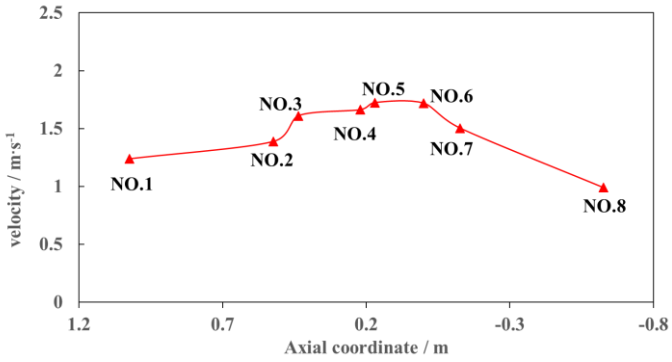

Fig. 6. Average axial transportation velocity of rock debris on each section (30 L/s, 60 r/min)

V. CONCLUSION

(1) Based on the CFD-DEM coupling technique, the simulation of the interaction between rock debris and drilling fluids, rock debris, and solid walls is realized, which provides a feasible numerical simulation method for the analysis of the flow field at the bottom of the well of the rock debris bed remover.

(2) Gravity is the main factor and obvious effect of rock debris settlement and rock debris bed accumulation, while the spiral structure of the rock debris bed remover has obvious rotary excavation effect on the rock debris at the bottom of the well as well as accelerating rock debris transportation, which can directly form the destruction of the rock debris bed.

(3) Compared with conventional drill pipes, the rock debris bed remover not only destroys the generation of rock debris beds, but also directly improves the rock-carrying performance of the flow field at the bottom of the well.

ACKNOWLEDGMENT

This work was supported by the Innovation and Entrepreneurship Training Program for College Students in Sichuan Province, China (NO. S202211116035) and the Scientific Research Project of Chengdu Technological University, China (NO. 2021ZR004 & NO. 2022ZR020).

REFERENCES

[1] K.L. Johnson, “Contact mechanics,” Cambridge: Cambridge University Press, 1987: 45-53.

[2] A.D. Renzo and F.P.D. Maio, “Comparison of contact-force models for the simulation of collisions in DEM-based granular flow codes,” Chemical Engineering Science, 2004, 59(3):525-541.

[3] S.B. Kuang and A.B. Yu, “Computational study of flow regimes in vertical pneumatic conveying,” Industrial & Engineering Chemistry Research, 2009, 48(14):6846-6858.

[4] Pham, V. Chi and R.W. Ogden, “On formulas for the Rayleigh wave speed,” Wave Motion, 2004, 39:191-197.

[5] Y.C. KUANG, R. ZHANG and J.W. LUO, “Numerical Simulation of Downhole Particle Flow in Horizontal Well with PDC Bit,” China Petroleum Machinery, 2019,47(07):36-42.